Design of a Magnetic Resonance-Safe Haptic Wrist Manipulator for Movement Disorder Diagnostics

Dyon Bode[1,2]
Moog B.V.,
Pesetaweg 53,
Nieuw-Vennep 2153 PJ, The Netherlands
e-mail: dbode@moog.com

Winfred Mugge[2]
Department of Biomechanical Engineering,
Faculty of Mechanical,
Maritime and Materials Engineering,
Delft University of Technology,
Mekelweg 2,
Delft 2628 CD, The Netherlands;
Brain Imaging Center,
Academic Medical Center,
Meibergdreef 9,
Amsterdam-Zuidoost 1105 AZ, The Netherlands
e-mail: w.mugge@tudelft.nl

Alfred C. Schouten
Department of Biomechanical Engineering,
Faculty of Mechanical,
Maritime and Materials Engineering,
Delft University of Technology,
Mekelweg 2,
Delft 2628 CD, The Netherlands;
Department of Biomechanical Engineering,
MIRA,
University of Twente,
Drienerlolaan 5,
Enschede 7522 NB, The Netherlands
e-mail: a.c.schouten@tudelft.nl

Anne-Fleur van Rootselaar
Department of Neurology and Clinical Neurophysiology,
Academic Medical Center,
University of Amsterdam,
Meibergdreef 9,
Amsterdam-Zuidoost 1105 AZ, The Netherlands;
Brain Imaging Center,
Academic Medical Center,
Meibergdreef 9,
Amsterdam-Zuidoost 1105 AZ, The Netherlands
e-mail: a.f.vanrootselaar@amc.uva.nl

Lo J. Bour
Department of Neurology and Clinical Neurophysiology,
Academic Medical Center,
University of Amsterdam,
Meibergdreef 9,
Amsterdam-Zuidoost 1105 AZ, The Netherlands
e-mail: bour@amc.uva.nl

Frans C. T. van der Helm
Department of Biomechanical Engineering,
Faculty of Mechanical,
Maritime and Materials Engineering,
Delft University of Technology,
Mekelweg 2,
Delft 2628 CD, The Netherlands
e-mail: f.c.t.vanderhelm@tudelft.nl

Piet Lammertse
Moog B.V.,
Pesetaweg 53,
Nieuw-Vennep 2153 PJ, The Netherlands
e-mail: piet.lammertse@motekforcelink.com

Tremor, characterized by involuntary and rhythmical movements, is the most common movement disorder. Tremor can have peripheral and central oscillatory components which properly assessed may improve diagnostics. A magnetic resonance (MR)-safe haptic wrist manipulator enables simultaneous measurement of proprioceptive reflexes (peripheral components) and brain activations (central components) through functional magnetic resonance imaging (fMRI). The presented design for an MR-safe haptic wrist manipulator has electrohydraulic closed-circuit actuation, optical position and force sensing, and consists of exclusively nonconductive and magnetically compatible materials inside the MR-environment (Zone IV). The MR-safe hydraulic actuator, a custom-made plastic vane motor, is connected to the magnetic parts and electronics located in the shielded control room (Zone III) via hydraulic hoses and optical fibers. Deliberate internal leakage provides backdriveability, damping, and circumvents friction. The manipulator is completely MR-safe and therefore operates safely in any MR-environment while ensuring fMRI imaging quality. Undesired external leakage in the actuator prevented the use of prepressure, limiting the control bandwidth. The compact end effector design fits in the MR-scanner, is easily setup, and can be clamped to the MR-scanner bed. This enables use of the manipulator with the subject at the optimal fMRI location and allows it to be setup quickly, saving costly MR-scanner time. The actuation and sensor solutions performed well inside the MR-environment and did not deteriorate image quality, which allows for various motor control experiments. Enabling prepressure by carrying out the recommendations on fabrication and sealing should improve the bandwidth and fulfill the requirements for proprioceptive reflex identification. [DOI: 10.1115/1.4037674]

Introduction

Movement disorders impair a person's ability to produce and control bodily movements [1]. Tremor, with a prevalence of 14.5% [2], is the most common movement disorder and characterized by involuntary, rhythmical movement of a body part [3]. Diagnosis can be difficult since there are many types of tremor, which arise from a range of neurological disorders.

Motor control is regulated by the central nervous system. The peripheral nervous system transports the motor commands and sensory feedback, respectively, from and to the central nervous system. Peripheral reflexes are fast involuntary movements in response to sensory feedback. When the frequency of the tremor depends upon the inertial and elastic properties of the limb and its load, then it has at least, in part, a peripheral reflex component,

[1]Corresponding author.
[2]D. Bode and W. Mugge contributed equally to this work.
Manuscript received November 7, 2016; final manuscript received August 7, 2017; published online October 4, 2017. Assoc. Editor: Michael Eggen.

which means that the tremor is produced by the oscillations in peripheral feedback loops. When the frequency of the tremor is independent of the peripheral feedback loop properties, i.e., not influenced by elastic and inertial loading, then it is considered a central neurogenic tremor and believed to originate from an oscillating neural network within the brain [4]. A tremor can thus have two oscillatory components, a peripheral reflex component and a central neurogenic component [5].

Early and precise diagnosis of tremor is crucial for the correct and thus most effective treatment. Yet, currently the clinical diagnosis of tremor is limited, subjective and fails to include the peripheral and central oscillation components, while analyses exist for both. The central neurogenic component can be analyzed using brain imaging techniques such as functional magnetic resonance imaging (fMRI), a technique based on magnetic resonance imaging that noninvasively visualizes oxygen consumption related to brain activity using strong magnetic fields and radio frequency pulses. The peripheral reflex component can be analyzed with a force-controlled haptic manipulator, which allows for unambiguous motor tasks and application of continuous random force perturbations. Such perturbations feel natural to the subject and evoke the use of proprioceptive reflexes. The haptic manipulator can then measure the response of the subject to these perturbations to identify the joint's endpoint admittance: the causal, dynamic relationship between a force (input) and position (output). Subsequently, closed-loop system identification techniques and neuromuscular modeling are used to quantify the reflexes [6–8]. To our knowledge, there is no commercially available manipulator applicable during fMRI that satisfies the requirements for proprioceptive reflex identification, the most stringent requirement being the perturbation bandwidth. There are several research projects that have produced manipulators intended for use during magnetic resonance imaging which use electric-based actuators [9–13], pneumatic actuators [14–17], hydraulic actuators [18,19], electrorheological fluid actuators [20], or mechanical transmission-based actuators [21,22]. Piezoelectric motors are often used when the magnetic resonance (MR) robotic manipulator is mostly stationary and does not require high bandwidth. Piezoelectric motors are compact and do not require and are not affected by a magnetic field, while they deliver high torque at low speed with high responsiveness and controllability. However, the mechanical transmission solutions and piezoelectric motors use electrical conductive materials and piezoelectric motors even electrically active components. Use of electrical conductive materials or electrically active components (non MR-safe) may compromise fMRI image quality. With the exception of the master–slave hydraulic actuation [18], the listed solutions have insufficient bandwidth and are not MR-safe. Yet, to mount the master–slave hydraulic actuator, a large and cumbersome non MR-safe frame is used. The use of the frame and the size of the actuator both prevent use of the device beside a person in the MR-scanner bore, impeding the placement of the subject's head in the optimal fMRI location, i.e., center of the MR-scanner bore.

Problem Statement. Since the central and peripheral oscillation tremor components influence each other (closed loop), the best way to investigate tremor is by measuring both components simultaneously using fMRI and a haptic manipulator. Yet, fMRI is sensitive to magnetic disturbances and uses a strong magnetic field, disallowing the use of electrical conductive or magnetic materials in the haptic manipulator. Current commercially available haptic manipulators do not comply with the requirements for proprioceptive reflex identification during fMRI and noncommercial custom built haptic manipulators from literature leave room for improvement.

Goal. The goal was to design an MR-safe haptic wrist manipulator capable of proprioceptive reflex identification.

Design

In literature, the term MR-compatible is often used to indicate the use of a device is meant for in an MR-environment (American College of Radiology (ACR) Safety Zone IV). However, since 2005, this term has no value regarding safe use in an MR-environment and is often misinterpreted and incorrectly used [23]. The Food and Drug Administration recognized American Society for Testing and Materials standard F2503 [24] defines the terms MR-safe, MR-conditional, and MR-unsafe. An item that has demonstrated to pose no known hazards in a specified MR-environment with specified conditions of use is MR-conditional. A device is deemed MR-safe when it poses no known hazards in any MR-environment [25]. In practice, MR-safe means that the manipulator is constructed from electrical nonconductive and magnetically compatible materials, such as plastics, glass, or rubber. Choosing to make the manipulator MR-safe instead of just MR-conditional ensures fMRI quality and makes it suited for safe use in any MR-environment, i.e., independent of facility, MR-scanner features, or MR scan parameters.

Requirements. Strict requirements that have to be met:

- Pose no hazard risks, be MR-safe, not cause image artifacts or deteriorate fMRI image quality, and have an emergency stop button.
- Allow for one degree-of-freedom wrist flexion and extension with physical limitation to range of motion [18,26].
- Allow for use in an MR-scanner bore of 1.5–2 m long and 60 cm in diameter [27]. The width available to the side of a person is approximately 120 mm [22]. Have a setup (donning and doffing) time of less than 10 min.
- Comfortably and safely clamp the forearm to isolate movement of the wrist.
- Move fast and smoothly with a torque delivery of at least 1.2 N·m, sufficient to accelerate the wrist, and perturb a contracted wrist [28].
- Measure angle and torque across the full range with at least 12-bit resolution and sample frequency of 200 Hz to enable force-controlled interaction with a human [29].

Preferred requirements that can be compromised on in decreasing order of importance:

- Attain a bandwidth of at least 20 Hz. All dynamics of a human arm are excited under 20 Hz [18,30], since the eigenfrequency of a (co-) contracted human wrist is approximately 15 Hz [26].
- Allow for 60 deg range of motion. Meaning 30 deg in both the flexion and extension directions from the neutral position (0 deg wrist angle).
- Achieve the sensation of moving freely through inertia and dynamic friction of less than 4.3 g m^2 and 0.21 N·m, respectively [28].
- Independence of MR facility and scanner features.
- Cost effective.

Actuation Solution. Conventional electromagnetic motors cannot be used in an MR-environment [31]. Due to the limited space available in the bore of an MR-scanner or due to MR incompatibility, actuation solutions are often used in combination with a transmission such that the actuator can be placed outside the bore or even the MR-environment. This allows for larger actuators and prevents image artifacts. On the other hand, the distance from the shielded control room (ACR Safety Zone III) to MR-scanner bore can easily reach 9 m, and a transmission will introduce friction, backlash, elasticity, and time delays depending on the type of transmission [9,22,32]. The transmission of the force or torque created by an actuator can be achieved with a belt, linkage, or shaft system. These systems have facility-specific designs and

Table 1 Assessment of actuation solutions from the literature: + fulfilled requirement and − unfulfilled requirement

	Requirement			
Actuation solution	MR-safe and fMRI quality	Bandwidth	Smooth motion	Torque
Hydraulic master–slave system[a]	+	+	+	+
Hydraulic/pneumatic valve systems[b]	+	−	+	+
Pneustep (pneumatic step motor)[c]	+	−	−	−
Bowden cables[d]	−	−	−	+

[a]Reference [18].
[b]Reference [32].
[c]Reference [15].
[d]Reference [21].

Table 2 Assessment of sensing solutions from the literature: + fulfilled requirement and − unfulfilled requirement

	Requirement			
Sensing solution	MR-safe and fMRI quality	Bandwidth	Position sensor	Torque sensor
Hydraulic sensor[a]	+	−	−	+
Fiber optic light intensity measurement[b]	+	+	+	+

[a]Reference [34].
[b]References [12,14,18,32,35], and [36].

therefore lack flexibility. The hydraulic master–slave actuation seems to be best suited for our application given the requirements (Table 1).

Sensing Solution. Conventional strain gauges cannot be used, since they comprise non-MR-compatible electronic and material parts. Previously, electrically active sensors made out of MR-compatible materials have been used inside the MR-environment. With the proper precautions, i.e., shielding and sufficient distance from the imaging area, image artefacts and noise can be kept at an acceptable level [20,33]. However, this means that the sensor needs to be tested for every imaging sequence and MR-scanner. To prevent electromagnetic interference and ensure the sensors compatibility with any imaging sequence, it is best to use a sensor without electrical components or wiring inside the MR-environment. The sensing solution requires transmission of sensor data that separates the electronics from the MR-safe parts, similar to the actuation. The sensor solution must be suited to create both a position and a torque sensor. Table 2 shows that the fiber optic light intensity measurement principle is suited to create torque and position sensors within our requirements.

Based on the requirements and best suited design solutions, MR-safe position and torque sensors and an MR-safe hydraulic vane motor were required. These parts were not commercially available and needed to be designed and custom-made.

Actuator: Hydraulic Vane Motor. The actuator design is based on the closed-circuit hydraulic master–slave solution [18]. In our case, a vane motor (slave) with hydraulic pump (master) is used instead of the cylinder–piston (Fig. 1). A vane motor is a fluid-powered actuator that converts a fluid pressure or flow into an angular displacement or torque.

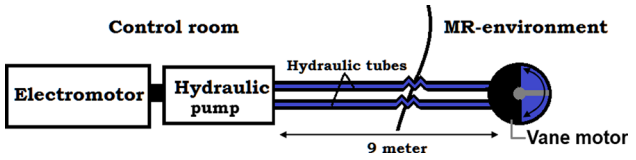

Fig. 1 Schematic representation of the hydraulic master–slave actuation system. The vane motor acts as the slave in the MR-environment, and the hydraulic pump, driven by an electromotor, acts as the master in the control room.

The first advantage of using a vane motor over a cylinder–piston configuration is that it is more compact and less complex, since it directly gives a rotational motion, circumventing additional equipment to convert linear motion into rotation. The second advantage is that a vane motor allows for internal leakage across the rotor. Internal leakage in the piston–cylinder configuration would make the master and slave piston go out of sync, since the master side cannot compensate for the leaking. This is not a problem with a vane motor, since the hydraulic pump has no constraints with regards to pumping fluids in either direction.

As creating a completely internal leakage free vane motor is impossible without strenuous sealing and thus considerable friction, we chose to design a vane motor that is allowed to have some internal leakage around the rotor, providing backdriveability and damping. Due to the internal leakage, a larger pump discharge and a position sensor on the rotor are required, but there is no longer any need for additional sealing between the rotor and the stator, which makes design and assembly easier as well as reducing friction and enabling smooth motion.

The vane motor had a double vane so that the axis of the rotor was loaded with a couple instead of a moment, resulting in less deformation of the rotor axis and thus less friction. The vane motor (Fig. 2) is designed to deliver 8 N·m at a 3 bar pressure difference and has a range of motion of 134 deg.

Sensors: Light Intensity Measurement. Fiber optics provide an MR-safe transmission of signals and have simple and flexible installation and negligible signal loss or time delays over long distances [12,14,32,35–37]. The light intensity principle to measure displacement can be applied using opposing fibers or a reflective surface. The advantage of using a reflective surface is that the emitting and receiving fiber are on the same side of the sensor and can share the same sensor head, guaranteeing alignment of the fibers.

Torque Sensor. The torque sensor (Fig. 3, top panel) consists of an optical sensor and a deformable body. The deformation of this body is detected using the knife-edge method. The sensor head (Keyence FU-38) is made out of plastics and is connected to

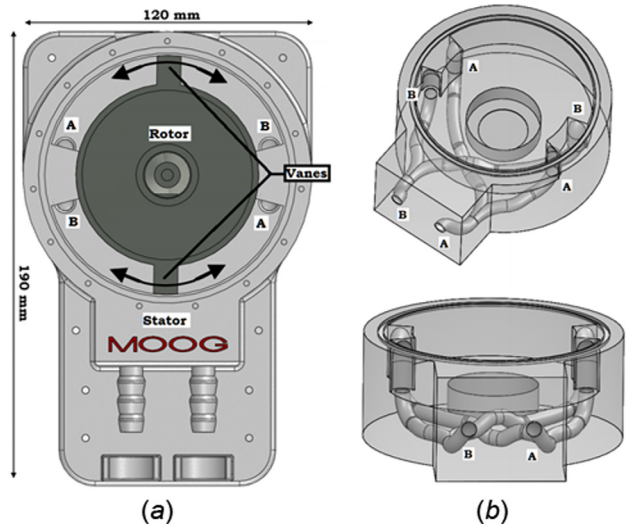

Fig. 2 Drawings of the vane motor. Coupled cross-linked fluid in/outlets are labeled either A or B. (*a*) Top view drawing of the vane motor with cover removed. (*b*) Transparent drawing of the base stator illustrating the cross-linked fluid ducts.

the amplifier (Keyence FS-N11MN) through optical fibers. The slot for the handle in the sensor body allows precise alignment of the wrist joint with the axis of the actuator.

Position Sensor. The position sensor (Fig. 3, bottom panel) uses a plastic sensor head (Keyence FU-37) also connected to an amplifier (Keyence FS-N11MN). A disk with an eccentric hole is placed on the axis of the vane motor and acts as an encoder disk. The rotation of the axis changes the area of reflective surface and thus acts as a unique reference for each position, resulting in absolute position sensing.

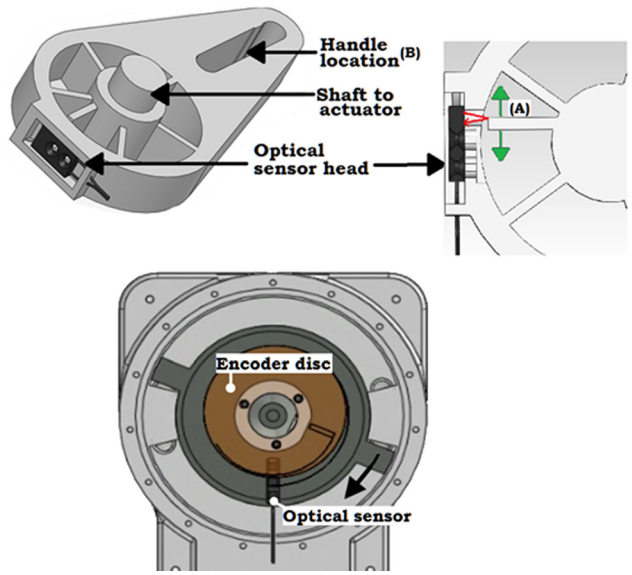

Fig. 3 The top panel shows drawings of the torque sensor with the knife-edge method to detect the displacement of (A) with regards to the sensor head when a force is applied to (B). The bottom panel shows a top view drawing of the absolute optical position sensor. In this rendering, the encoder disk is made transparent so that the optical sensor can be seen. Rotor direction of motion is indicted by the arrow. The position sensor is in one extreme resulting in the minimal amount of reflective surface from the encoder disk.

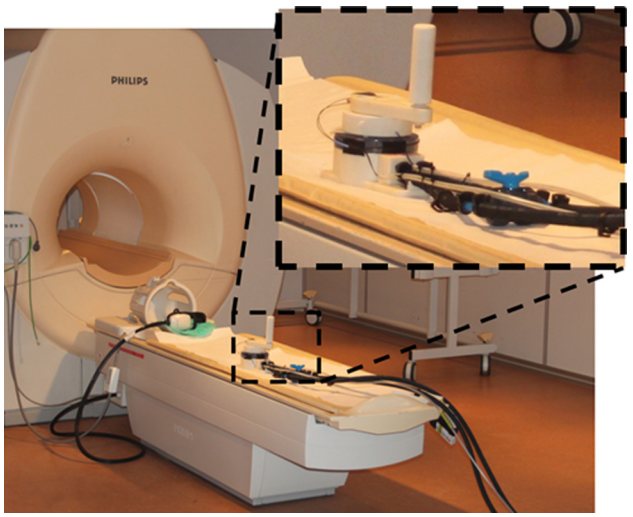

Fig. 4 Photograph of the MR-safe haptic wrist manipulator inside the MR-environment, showing the vane motor, optical sensors, and 9 m hoses. Note that the real-time computer, electromotor and drive, hydraulic pump, reservoir and valves, and emergency stop button are outside the MR-environment in the control room.

Complete System Prototype. The parts for the prototype of the MR-safe haptic wrist manipulator are manufactured out of three materials and manufactured using rapid prototyping techniques (Fig. 4).

The prototype for the actuator is built using a Moog servo drive (G392-008) and electric motor (C-100). The electric motor is connected to a hydraulic reversible gear pump (Galtech 2SM-A-4-R) with a displacement of 4 cc/rev. The 9 m long hoses connecting the hydraulic pump and vane motor consist of a synthetic rubber inner (3/8 in) and outer mantle with two woven fabric inlays (Hebu 0503-06). A hydraulic fluid vegetable oil is used because of its nontoxic, noncorrosive nature, and easy availability. The real-time computer controls the system and samples the torque and position at a sample frequency of 2048 Hz with a 16-bit resolution.

Control. The real-time computer uses a virtual model and controls the velocity of the actuator with a proportional–integral (PI) controller and an additional parallel feed-forward gain (K_{leak}) to compensate for the internal leakage of the vane motor. K_{leak} was determined by applying different static torques to the handle and measuring the expired time for a certain rotational translation ($K_{leak} = 0.3$ rad/(N·m s)). In an attempt to further increase the control performance, an additional gain (K_{fric}) related to the motion direction was added to compensate for the static coulomb friction, which was determined to be 0.14 N·m.

Results

To investigate the performance of the MR-safe haptic wrist manipulator prototype, several tests were performed to determine the accuracy of the optical sensors and maximum actuator torque. For the characterization of the system, the open-loop frequency response function (FRF) of the commanded velocity to the vane velocity was measured. Additionally, the ability to identify the impedance FRFs of two inertial loads, i.e., the handle and the handle with a mass, was tested. As a final test in an MR-scanner (3T Philips Intera, Best, The Netherlands), the manipulator operated as expected, showing no distortions in the MR-image or in the prototype's sensor signals as only MR-safe materials where used inside the MR-environment.

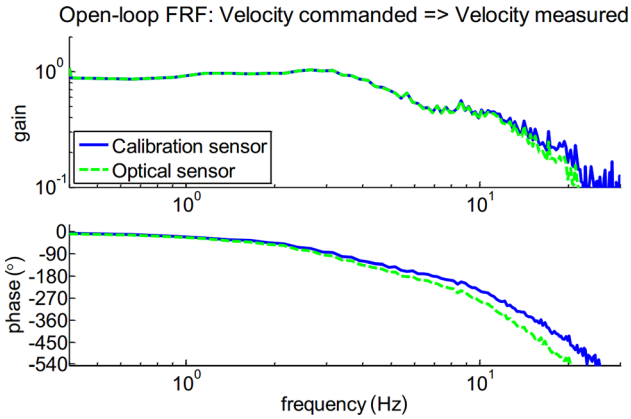

Fig. 5 The open-loop FRFs of the commanded velocity to the measured vane velocity. The dashed trace represents the FRF as determined with the optical sensor; for comparison, the solid trace represents the FRF determined with the calibration sensor. The FRF made with the measurements from the optical sensor has an increased phase lag due to filtering.

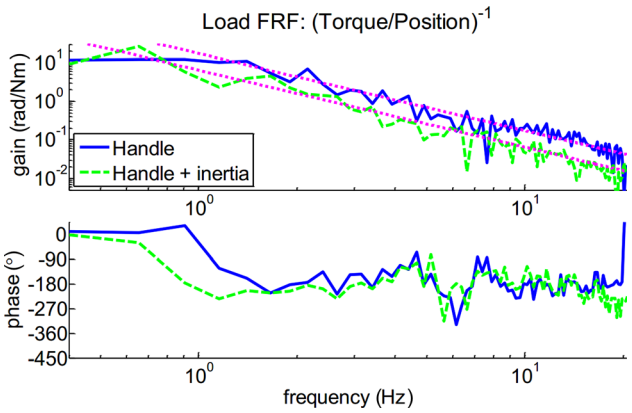

Fig. 6 The closed-loop FRFs of the measured torque to the commanded position. The dotted traces represent the fitted inertias.

Optical Position Sensor. The prototype MR-safe optical position sensor has a measurement range of 70 deg and was calibrated using a potentiometer (Feteris FCP 12AC) with a voltage output smoothness of 0.1% against input voltage and sampled with a 16-bit analog to digital converter. After the calibration, the measured position of the optical sensor was compared to the measured position of the calibration sensor in a test that was repeated five times. The maximum deviation of the position measured with the optical sensor in respect to the calibration sensor is ±1% full scale (F.S. = 70 deg).

Optical Torque Sensor. The MR-safe optical torque sensor prototype was statically calibrated using a pulley that ensured loading of the torque sensor at a moment arm of 91 mm. The calibration test was repeated four times, and the results showed an accuracy of ±2% full scale (F.S. = 14.3 N·m).

Maximum Torque. The maximum torque that could be produced with the prototype actuator was determined by fixating the handle. Several measurements were performed in which the pump velocity was increased until the maximum measured torque was reached, which was 1.5 N·m.

Open-Loop FRF. The electric motor is velocity controlled by its servo controller. To determine the system characteristics, the open-loop FRF of the commanded velocity to the measured vane velocity was determined. The commanded velocity input signal was a 30 s multisine with uniformly distributed power between 0.1 and 30 Hz [38]. To exclude transient effects, the first and last 7 s were removed, leaving a 16 s signal for analysis. The FRF (Fig. 5) is the spectral density of the measured vane velocity divided by the spectral density of the commanded velocity, based on a five repetitions average of velocity measurements and smoothed by averaging over four adjacent frequency bands. The open-loop bandwidth is ~5 Hz (−3 dB, i.e., a gain of 0.707).

Impedance FRF. The system's capability to identify inertial loads was tested by analyzing the impedance from the commanded position multisine disturbance and the measured position and torque for two inertial loads: 1.46 g m^2 (handle inertia) and 3.93 g m^2 (handle + mass of 480 g). The inertias of the handle and load were calculated with the use of a SOLIDWORKS model. The closed-loop FRFs were calculated from spectral densities using closed-loop system identification [26]. The FRFs show typical second-order responses with a smaller admittance or larger impedance for the greater inertial load (Fig. 6). Hand calculations to determine the inertia of the loads from the FRFs were performed and yielded estimated inertias of 1.5 g m^2 and 4.3 g m^2 for, respectively, the handle (1.46 g m^2) and the handle with a load (3.93 g m^2).

Discussion

This paper presents a design for an MR-safe haptic wrist manipulator suited for proprioceptive reflex identification. After the design phase, a proof-of-concept prototype was made which resulted in a custom-made MR-safe prototype with electrohydraulic actuation, an optical position sensor, and an optical torque sensor. All materials used inside the MR-environment (Zone IV) are electrically nonconductive, nonmetallic, and nonmagnetic.

The design splits the manipulator into an MR-safe and MR-unsafe part, connecting the MR-safe hydraulics and sensors via 9 m of hydraulic hoses and optical fibers to the magnetic and electronics parts of the system in the shielded control room (Zone III).

MR-Safe. Whether a material is MR-safe is debatable because of how it is determined [23]. An item is deemed MR-safe by providing a scientifically based rationale rather than test data. This means that conducting magnetic compatible materials, such as aluminum, which are not susceptible to induced force or torques but are susceptible to induced eddy currents are cause for debate [24,25,29]. Induced eddy currents can cause heating of the material (safety hazard) and a local magnetic field, which deteriorates fMRI image quality. Therefore, conducting magnetically compatible materials are not MR-safe. However, when conducting magnetically compatible materials are used outside the bore, on nonmoving parts, and it is impossible for the subjects to become part of a conductive loop, then there is no direct safety hazard and image quality is not necessarily compromised. Nevertheless, to avoid discussion, in this design only electrical nonconductive and nonmagnetic compatible materials were used. As a result, the fMRI quality is ensured, and the manipulator is suited for safe use in any MR-environment.

Material, Production Technique, and Sealing. There was some undesired external leakage along the axis of the vane motor, possibly caused by the limited shape accuracy of rapid prototyping techniques or the finish of the materials. Other fabrication techniques can provide a higher accuracy; however, the internal ducts of the vane motor exclude many other production techniques. A possible solution would be to use rapid prototype techniques with oversized part dimensions so that finishing can be performed with conventional milling machines and lathes to improve the accuracy.

Maximum Torque. The vane motor was unable to deliver its designed torque at a pressure difference of 3 bar because of cavitation. Without prepressure, the pressure at the inlet pump became too low, resulting in a free turning pump. This limited the achieved torque to 1.5 N·m, which still was enough to meet the requirement of 1.2 N·m.

Sensors. The sensors in the prototype have extended fibers to reach a length of 9 m total, the maximum length available from the manufacturer was 5 m. However, not needing an extension coupling is preferable, since it decreases the risk of signal distortions. The lead time for a specialized custom fabrication of the used sensor heads with fibers of 9 m long was too long for use in this research.

The workspace of the system was limited to 70 deg (i.e., −35 deg to 35 deg) by the position sensor encoder disk dimensions instead of the vane motor workspace of 134 deg. At the ends of the range of motion, the position sensor became inaccurate. To increase the range of motion, the usable reflective surface of the encoder disk needs to be redistributed over a larger range. For the assessment of the manipulator, the currently achieved workspace of 70 deg fulfilled the requirement. The design used for the encoder disk is a circle with an eccentric hole. This results in a nonlinear distribution of the reflective surface over the range of motion. Instead of a circle, a specific curved shape provides a linear distribution of the reflective surface over the range of motion. However, since the fabrication of such a curved shape requires the use of an x–y table, it will result in an edge with discrete steps. For the prototype, a circle was chosen as encoder disk because it can be constructed on a lathe, which results in a continuous edge. The nonlinear distribution of reflective surface was accounted for in the control software of the system.

Control. Controlling the system accurately over the desired bandwidth (20 Hz) with a PI controller was not successful due to the inherent nonlinearities of hydraulics such as cavitation. Attempts to improve control performance by adding a parallel feed-forward gain to the commanded velocity to compensate for the internal leak of the vane motor and a compensation gain for the static coulomb friction improved performance, but did not fully resolve the issues. When tuning the PI controller, accurate position tracking for 1 and 2 Hz sine waves was achieved, without signs of stick–slip friction. Prepressure will likely solve many of the control issues, if not, then implementation of model-based control will likely improve the control performance of the system and achieve a higher bandwidth.

Conclusion

The main challenge was to design and build a manipulator that would function safely in any MR-environment (Zone IV) during fMRI without compromising the image quality. During a test in an MR-scanner, no distortions in the MR-image and no distortions in the sensor signal were observed using electrohydraulic actuation in the control room (Zone III) and MR-safe optical sensors, hydraulic hoses, and a custom-made vane motor (end effector) inside the MR-environment. The one degree-of-freedom MR-safe wrist manipulator prototype achieved smooth motion without stick–slip over a range of motion of 70 deg (i.e., −35 deg to 35 deg), produced a torque of 1.5 N·m, and is easily setup, fulfilling all but one of the requirements. The performance of the prototype was limited by undesired external leakage across the vane motor axis, which prevented the use of prepressure.

Without prepressure, the open-loop FRF of the commanded velocity to the measured vane velocity had a reducing gain from ∼5 Hz. Although the bandwidth does not fulfill the requirement for proprioceptive reflex identification, it does allow for various motor control experiments and enabled identification as inertial loads were accurately estimated using closed-loop identification.

The, in this paper, described system is one of the few [16,18,19,21] capable of producing fast and smooth motion. However, the system described is the only one being fully MR-safe. The parts in the MR-environment are easily connected to the rest of the system by two hydraulic and two fiber optic connections. The system by Gassert et al. [18] does achieve a bandwidth of 20 Hz and comes close to the MR-safe requirement by using MR-safe components with the exception of an aluminum frame to hold the system. The system differs further from Gassert et al. [18] by having an absolute position sensor and a more compact end effector design which fits beside a person in the MR-scanner bore and can be clamped to the MR-scanner bed. These improvements enable use of the manipulator with the subject at the optimal fMRI location in the MR-scanner bore and allow it to be setup in little time which saves costly MR-scanner time. With the recommendations carried out, proprioceptive reflex identification during fMRI should be achievable.

Recommendations

Prepressure. The next steps for the MR-safe haptic manipulator will be to improve the bandwidth and maximum torque by making prepressure possible. Therefore, the undesired external leakage around the axis must be remedied with different or additional fabrication techniques to improve the accuracy of the parts. Furthermore, the preferred sealing for low-pressure dynamic rotary movement is a lip-seal, which could not be used since they have a metal housing. Hence, the feasibility of a custom-made lip-seal constructed out of plastic should be explored.

Applications. Proprioceptive reflex identification is motor control research with one of the most stringent demands regarding the haptic manipulator. Besides proper tremor diagnosis, combining an MR-scanner and the MR-safe haptic manipulator allows for other motor control research (e.g., sensory weighting, perturbed posture, and goal-directed motions). Investigating how the brain changes over time while learning a motor task improves the understanding of brain circuits involved in normal motor learning and in cortical remapping [39,40]. The combination of fMRI and proprioceptive reflex identification will potentially provide insight into brain functions, functional and dysfunctional motor control, and the regeneration process after a nerve lesion, making this combination of techniques an interesting tool for neuroscientists and technicians [32,41,42].

Acknowledgment

This research is part of the NeuroSIPE program and is funded by the Dutch Technology Foundation STW (STW Grant No. 10739: The Movement Diagnostic System), which is part of the Netherlands Organization for Scientific Research (NWO) and partly funded by the Ministry of Economic Affairs, Agriculture and Innovation. Research supported by STW NeuroSIPE Project No. 10739: The Movement Diagnostic System (MDS).[3]

Special thanks to Paul F. C. Groot (Radiology department, Academic Medical Center, Amsterdam) for all his help related to measurements in the MR-environment.

Funding Data

- Stichting voor de Technische Wetenschappen (Grant No. 10739).

References

[1] Chou, K. L., Grube, S., and Patil, P. G., 2012, *Deep Brain Stimulation: A New Life for People With Parkinson's, Dystonia, and Essential Tremor*, Demos Medical Publishing, New York.

[2] Wenning, G. K., Kiechl, S., Seppi, K., Müller, J., Högl, B., Saletu, M., Rungger, G., Gasperi, A., Willeit, J., and Poewe, W., 2005, "Prevalence of Movement

[3] http://neurosipe.nl/project.php?id=25

Disorders in Men and Women Aged 50-89 Years (Bruneck Study Cohort): A Population-Based Study," Lancet Neurol., **4**(12), pp. 815–820.
[3] Deuschl, G., Bain, P., and Brin, M., 1998, "Consensus Statement of the Movement Disorder Society on Tremor," Mov. Disord., **13**(S3), pp. 2–23.
[4] Elble, R. J., 1996, "Central Mechanisms of Tremor," J. Clin. Neurophysiol., **13**(2), pp. 133–144.
[5] Grimaldi, G., and Manto, M., 2008, *Tremor: From Pathogenesis to Treatment*, Morgan & Claypool, San Rafael, CA.
[6] Kearney, R. E., Stein, R. B., and Parameswaran, L., 1997, "Identification of Intrinsic and Reflex Contributions to Human Ankle Stiffness Dynamics," IEEE Trans. Biomed. Eng., **44**(6), pp. 493–504.
[7] Mirbagheri, M. M., Barbeau, H., and Kearney, R. E., 2000, "Intrinsic and Reflex Contributions to Human Ankle Stiffness: Variation With Activation Level and Position," Exp. Brain Res., **135**(4), pp. 423–436.
[8] van der Helm, F. C. T., Schouten, A. C., de Vlugt, E., and Brouwn, G. G., 2002, "Identification of Intrinsic and Reflexive Components of Human Arm Dynamics During Postural Control," J. Neurosci. Methods, **119**(1), pp. 1–14.
[9] Tsekos, N. V., Christoforou, E., and Özcan, A., 2008, "A General-Purpose MR-Compatible Robotic System," IEEE Eng. Med. Biol. Mag., **27**(3), pp. 51–58.
[10] Chinzei, K., Kikinis, R., and Jolesz, F. A., 1999, "MR Compatibility of Mechatronic Devices: Design Criteria," *Medical Image Computing and Computer-Assisted Intervention—MICCAI*, Springer, Berlin, pp. 1020–1030.
[11] Elhawary, H., Zivanovic, A., Rea, M., Davies, B. L., Besant, C., Young, I., and Lamperth, M. U., 2008, "A Modular Approach to MRI-Compatible Robotics," IEEE Eng. Med. Biol. Mag., **27**(3), pp. 35–41.
[12] Flueckiger, M., Bullo, M., Chapuis, D., Gassert, R., and Perriard, Y., 2005, "fMRI Compatible Haptic Interface Actuated With Traveling Wave Ultrasonic Motor," IEEE Industry Applications Conference, 40th IAS Annual Meeting, Hong Kong, China, Oct. 2–6, pp. 2075–2082.
[13] Yamamoto, A., Ichiyanagi, K., Higuchi, T., Imamizu, H., Gassert, R., Ingold, M., Sache, L., and Bleuler, H., 2005, "Evaluation of MR-Compatibility of Electrostatic Linear Motor," IEEE International Conference on Robotics and Automation (ICRA), Barcelona, Spain, Apr. 18–22, pp. 3658–3663.
[14] Yu, N., Murr, W., Blickenstorfer, A., Kollias, S., and Riener, R., 2007, "An fMRI Compatible Haptic Interface With Pneumatic Actuation," IEEE Tenth International Conference on Rehabilitation Robotics (ICORR), Noordwijk, The Netherlands, June 13–15, pp. 714–720.
[15] Stoianovici, D., Patriciu, A., Petrisor, D., Mazilu, D., and Kavoussi, L., 2007, "A New Type of Motor: Pneumatic Step Motor," IEEE/ASME Trans. Mechatron., **12**(1), pp. 98–106.
[16] Diedrichsen, J., Hashambhoy, Y., Rane, T., and Shadmehr, R., 2005, "Neural Correlates of Reach Errors," J. Neurosci., **25**(43), pp. 9919–9931.
[17] Suminski, A. J., Zimbelman, J. L., and Scheidt, R. A., 2007, "Design and Validation of a MR-Compatible Pneumatic Manipulandum," J. Neurosci. Methods, **163**(2), pp. 255–266.
[18] Gassert, R., Moser, R., Burdet, E., Bleuler, H., Member, S., Moser, R., and Burdet, E., 2006, "MRI/fMRI-Compatible Robotic System With Force Feedback for Interaction With Human Motion," IEEE/ASME Trans. Mechatron., **11**(2), pp. 216–224.
[19] Yu, N., Estévez, N., Hepp-Reymond, M. C., Kollias, S. S., and Riener, R., 2011, "FMRI Assessment of Upper Extremity Related Brain Activation With an MRI-Compatible Manipulandum," Int. J. Comput. Assist. Radiol. Surg., **6**(3), pp. 447–455.
[20] Khanicheh, A., Muto, A., Triantafyllou, C., Weinberg, B., Astrakas, L., Tzika, A., and Mavroidis, C., 2006, "fMRI-Compatible Rehabilitation Hand Device," J. Neuroeng. Rehabil., **3**(1), pp. 1–11.
[21] Chapuis, D., Gassert, R., Ganesh, G., Burdet, E., and Bleuler, H., 2006, "Investigation of a Cable Transmission for the Actuation of MR Compatible Haptic Interfaces," The First IEEE/RAS-EMBS International Conference on Biomedical Robotics and Biomechatronics (BioRob), Pisa, Italy, Feb. 20–22, pp. 426–431.
[22] Christoforou, E. G., Tsekos, N. V., and Özcan, A., 2006, "Design and Testing of a Robotic System for MR Image-Guided Interventions," J. Intell. Rob. Syst., **47**(2), pp. 175–196.
[23] Schaefers, G., 2008, "Testing MR Safety and Compatibility," IEEE Eng. Med. Biol. Mag., **27**(3), pp. 23–27.
[24] ASTM, 2008, "Standard Practice for Marking Medical Devices and Other Items for Safety in the Magnetic Resonance Environment," ASTM International, West Conshohocken, PA, Standard No. F2503-08.
[25] Kanal, E., Barkovich, A. J., Bell, C., Borgstede, J. P., Bradley, W. G., Froelich, J. W., Gilk, T., Gimbel, J. R., Gosbee, J., Kuhni-Kaminski, E., Lester, J. W., Nyenhuis, J., Parag, Y., Schaefer, D. J., Sebek-Scoumis, E. A., Weinreb, J., Zaremba, L. A., Wilcox, P., Lucey, L., Sass, N., and the ACR Blue Ribbon Panel on MR Safety, 2007, "ACR Guidance Document for Safe MR Practices: 2007," Am. J. Roentgenol., **188**(6), pp. 1447–1474.
[26] Schouten, A. C., de Vlugt, E., van Hilten, J. J. B., and van der Helm, F. C. T., 2006, "Design of a Torque-Controlled Manipulator to Analyse the Admittance of the Wrist Joint," J. Neurosci. Methods, **154**(1–2), pp. 134–141.
[27] Tsekos, N. V., Ozcan, A., and Christoforou, E., 2005, "A Prototype Manipulator for Magnetic Resonance-Guided Interventions Inside Standard Cylindrical Magnetic Resonance Imaging Scanners," ASME J. Biomech. Eng., **127**(6), pp. 972–980.
[28] Williams, D., 2001, *Robot for Wrist Rehabilitation*, MIT, Cambridge, MA.
[29] Gassert, R., Chapuis, D., Bleuler, H., and Burdet, E., 2008, "Sensors for Applications in Magnetic Resonance Environments," IEEE/ASME Trans. Mechatron., **13**(3), pp. 335–344.
[30] Perreault, E. J., Kirsch, R. F., and Crago, P. E., 2001, "Effects of Voluntary Force Generation on the Elastic Components of Endpoint Stiffness," Exp. Brain Res., **141**(3), pp. 312–323.
[31] Burdet, E., Gassert, R., Gowrishankar, G., Chapuis, D., and Bleuler, H., 2006, "fMRI Compatible Haptic Interfaces to Investigate Human Motor Control," Exp. Rob. IX, **21**, pp. 25–34.
[32] Yu, N., Hollnagel, C., Blickenstorfer, A., Kollias, S. S., and Riener, R., 2008, "Comparison of MRI-Compatible Mechatronic Systems With Hydrodynamic and Pneumatic Actuation," IEEE/ASME Trans. Mechatron., **13**(3), pp. 268–277.
[33] Hidler, J., Mbwana, J., and Zeffiro, T., 2005, "MRI Compatible Force Sensing System for Real-Time Monitoring of Wrist Moments During fMRI Testing," Ninth International Conference on Rehabilitation Robotics (ICORR), Chicago, IL, June 28–July 1, pp. 212–214.
[34] Liu, J. Z., Dai, T. H., Elster, T. H., Sahgal, V., Brown, R. W., and Yue, G. H., 2000, "Simultaneous Measurement of Human Joint Force, Surface Electromyograms, and Functional MRI-Measured Brain Activation," J. Neurosci. Methods, **101**(1), pp. 49–57.
[35] Chapuis, D., Gassert, R., Sache, L., Burdet, E., and Bleuler, H., 2004, "Design of a Simple MRI/fMRI Compatible Force/Torque Sensor," IEEE/RSJ International Conference on Intelligent Robots and Systems (IROS), Sendai, Japan, Sept. 28–Oct. 2, pp. 2593–2599.
[36] Hara, M., Matthey, G., Yamamoto, A., Chapuis, D., Gassert, R., Bleuler, H., and Higuchi, T., 2009, "Development of a 2-DOF Electrostatic Haptic Joystick for MRI/fMRI Applications," IEEE International Conference on Robotics and Automation (ICRA), Kobe, Japan, May 12–17, pp. 1479–1484.
[37] Vlaar, M. P., Mugge, W., Groot, P. F. C., Sharifi, S., Bour, L. J., van der Helm, F. C. T., van Rootselaar, A.-F., and Schouten, A. C., 2016, "Targeted Brain Activation Using an MR-Compatible Wrist Torque Measurement Device and Isometric Motor Tasks During Functional Magnetic Resonance Imaging," Magn. Reson. Imaging, **34**(6), pp. 795–802.
[38] Pintelon, R., and Schoukens, J., 2001, *System Identification: A Frequency Domain Approach*, Wiley-IEEE Press, New York.
[39] Tsekos, N. V., Khanicheh, A., Christoforou, E., and Mavroidis, C., 2007, "Magnetic Resonance–Compatible Robotic and Mechatronics Systems for Image-Guided Interventions and Rehabilitation: A Review Study," Annu. Rev. Biomed. Eng., **9**(1), pp. 351–387.
[40] Rowe, J. B., and Frackowiak, R. S. J., 1999, "The Impact of Brain Imaging Technology on Our Understanding of Motor Function and Dysfunction," Curr. Opin. Neurobiol., **9**(6), pp. 728–734.
[41] Gassert, R., Burdet, E., and Chinzei, K., 2008, "Opportunities and Challenges in MR-Compatible Robotics," IEEE Eng. Med. Biol. Mag., **27**(3), pp. 15–22.
[42] Heeger, D. J., and Ress, D., 2002, "What Does fMRI Tell Us About Neuronal Activity?," Nat. Rev. Neurosci., **3**(2), pp. 142–151.